NUMERICAL SIMULATION OF TRANSIENT TURBULENT COMPRESIBLE FLOW IN A NATURAL GAS PIPELINE

Effiong, E. E.[1], Orga, A. C.[1], Ibe, E. C.[1], [*]Ekeke, I. C.[1] and Nzebuka, C. G.[2]
[1] Chemical Engineering Department, [2] Materials and Metallurgical Engineering Department
Federal University of Technology, Owerri, Imo State, Nigeria
Author for correspondence; e-mail: ifyekeke@yahoo.com

ABSTRACT

Transient compressible natural gas flow through a pipeline was studied by the use of a finite volume method in 2D axisymmetric cylindrical coordinates. To account for turbulence within the pipeline system, the standard $k-\varepsilon$ *turbulence equations were modeled together with the Navier Stokes equations via the Reynolds-Averaged method. The equation of state employed was the Soave-Redlich-Kwong equation. The Pressure Implicit with Splitting of Operators (PISO) algorithm was then used for calculating the pressure and velocities on a staggered grid. Computer simulation was carried out to determine pressure variation, density variation, velocity variation and temperature variation within the pipeline system. The shapes of the profiles obtained from the results were in agreement with those obtained in validated literature results.*

Keywords: *Transient, compressible, cylindrical, axisymmetric, pipeline and turbulence.*

1. INTRODUCTION

Unsteady flow of natural gas in pipelines involves change of certain flow variables such as pressure, velocity, density, temperature with respect to time or distance as a result of disturbances in the system. The accurate prediction of these variables is therefore very important since this information gives the pipeline operator an insight into the behaviour of the system at any given point in time.

Many researchers in the past have modelled compressible flow in pipelines using various numerical methods. Siögreen (1995) employed the use of centered finite difference methods of general order of accuracy 2p to solve the compressible Navier-Stokes equations. Kessal et al (2014) analytically and numerically analysed a set of equations governing an isothermal compressible fluid flow in short pipeline. The equations were written in characteristics form and solved by a predictor-corrector lambda scheme for the interior mesh points. The method of characteristics was used for the boundaries. Accurate grid-converged results were obtained.

Behbahani-Nejad, et al (2008) presented an effective transient flow simulation based on the transfer function models and Matlab Simulink for gas pipelines and networks. In the paper by Nouri-Borujerdi (2011), simulation of transient 1D compressible adiabatic gas flows in a long pipeline following a catastrophic failure using a finite difference scheme was carried out. The advantages of this scheme are reduction of grid points, less computational effort and time with high accuracy. Noorbehesht (2012) modelled compressible natural gas flow in a transmission line at steady state in 2D cylindrical coordinates. The Navier Stokes equation, the ideal gas equation of state and the k-ε turbulence models were applied. A finite volume method, involving the SIMPLER algorithm (Patankar and Spalding, 1972; Patankar, 1980) was then used for the solution of the equations. Results obtained by this method agreed very well with experimental data obtained from the National Iranian Gas Company. An approximate 4% error proved the accuracy of this method. Finally, effect of variation in temperature of inlet gas, gas' flow rate, and ambient temperature on pressure drop and system's parameters were studied. In another paper, Noorbehesht, et al, (2013) investigated the dynamic behavior of natural gas in transmission line by same finite volume method applied earlier. The accuracy of this method was verified by comparing the experimental field data with this approach, showing errors of approximately 4 to 4.5%, which shows the precision of this approach. Finally, a case study was used as an application for the model and the best possible operating solution was proposed for a compressor station failure during winter. Nouri-Borujerdi et al (2007) investigated the numerical modeling of the dynamic behavior of compressible gas flow in pipelines by a finite-volume based finite-element method. The numerical simulation was performed by solving the coupled conservation form of the governing equations for 2D laminar, viscous, supersonic flows in the developing region under different thermal boundary conditions. The results indicated that heating the gas flow leads to an increase in pressure loss. Nouri-Borujerdi et al (2010) again presented a study on 2D unsteady turbulent compressible high pressure gas flow with a rupture at its center numerically. A computer code based on a mixed finite element-finite volume formulation for an unstructured grid was used to solve the problem. The turbulence modeling is based on the $k-\boldsymbol{\varepsilon}$ model, followed by a two layer technique near the wall. His results show that the numerical scheme employed is stable and accurate.

So many other works have been carried out by researchers which cannot be listed here. Most of these works have been done in Cartesian coordinates. Few have been carried out in cylindrical coordinates. This work therefore presents a finite volume method for solving 2D transient gas flow in cylindrical coordinates using the real gas Soave-Redlich Kwong equation of state. The finite volume method involves the use of the Pressure Implicit Scheme with Splitting of Operators to solve the Reynolds-Averaged Navier Stokes equation in 2D axisymmetric cylindrical coordinates. The $k-\boldsymbol{\varepsilon}$ turbulence model is incorporated to enable the prediction of turbulent eddy viscosity. To the authors' knowledge, no work has been published which employs this same method of simulation. To validate the model, pressure data published by Noorbehesht (2012) which he obtained from the National Iranian Gas Company for the validation of the model he proposed were used. The geometry of the pipeline he considered for simulation was scaled down for the purpose of this simulation and a scale factor obtained. This scale factor was then used to calculate the inlet and outlet pressures employed in the present work to obtain an accurate result for the pressure profile. The profile is similar to that obtained by Noorbehesht (2012). This proves the accuracy of the solution used for the model. Profiles for temperature, density, velocity along the pipeline were also obtained.

2. THE MATHEMATICAL MODEL

The basic equations used to model flow in pipelines and employed in this work are the compressible Navier-Stokes equations. In carrying out this work, it was assumed that the cross-sectional area of the pipe is constant. Another assumption made is that the gas flow is highly turbulent.

2.1 Conservation of mass or continuity equation: In its general form, the continuity equation is expressed as *(*Bird et al, 2002);

$$\frac{\partial \rho}{\partial t}+\frac{1}{r}\frac{\partial}{\partial r}(\rho r V_r)+\frac{\partial}{\partial z}(\rho V_z) = 0 \quad (1)$$

2.2 Conservation of Momentum equation in terms of $\boldsymbol{\tau}$ in the r and z-directions: For gas flows in a pipe, the compressible Navier-Stokes equations can be written for the axial and radial directions, respectively (Bird *et al.*, 2002) as;

$$\frac{\partial(\rho V_r)}{\partial t}+\frac{1}{r}\frac{\partial(r\rho V_r V_r)}{\partial r}+\frac{\partial(\rho V_r V_z)}{\partial z} = -\frac{\partial P}{\partial r}-\frac{1}{r}\frac{\partial}{\partial r}(r\tau_{rr})-\frac{\partial}{\partial z}\tau_{zr}+\frac{\tau_{\theta\theta}}{r} \quad (2)$$

$$\frac{\partial(\rho V_z)}{\partial t}+\frac{1}{r}\frac{\partial(r\rho V_r V_x)}{\partial r}+\frac{\partial(\rho V_z V_z)}{\partial z} = -\frac{\partial P}{\partial r}-\frac{1}{r}\frac{\partial}{\partial r}(r\tau_{zr})-\frac{\partial}{\partial z}\tau_{zz} \quad (3)$$

where

$$\tau_{rr} = -\mu_{eff}\left(2\frac{\partial V_r}{\partial r}-\frac{2}{3}(\nabla.v)\right) \quad (4)$$

$$\tau_{xz} = -\mu_{eff}\left(2\frac{\partial V_z}{\partial z}-\frac{2}{3}(\nabla.v)\right) \quad (5)$$

$$\tau_{xr} = -\mu_{eff}\left(\frac{\partial V_r}{\partial z}+\frac{\partial V_z}{\partial r}\right) \quad (6)$$

$$\tau_{\theta\theta} = -\mu_{eff}\left(2\frac{V_r}{r}-\frac{2}{3}(\nabla.v)\right) \quad (7)$$

$$\nabla.v = \frac{1}{r}\left(\frac{\partial}{\partial r}\right)(rV_r)+\frac{\partial V_z}{\partial z} \quad (8)$$

$\mu_{eff} = \mu+\mu_t = effective\ viscosity$ (Blazek, 2001)

2.3 Conservation of Energy Equation; The energy equation in its basic form in terms of temperature is;

$$\frac{\partial}{\partial t}(\rho c_p T) + \frac{\partial}{\partial z}(\rho c_p V_z T) + \frac{1}{r}\frac{\partial}{\partial r}(r\rho c_p V_r T) = \frac{\partial}{\partial z}\left(\left(\lambda + \frac{c_p \mu_t}{G_T}\right)\frac{\partial T}{\partial z}\right) + \frac{1}{r}\frac{\partial}{\partial r}\left(r\left(\lambda + \frac{c_p\mu_t}{G_T}\right)\frac{\partial T}{\partial r}\right) + S_T \quad (9)$$

2.4 Equation of State

The equation of state adopted in this work is the Soave-Redlich-Kwong equation stated as follows (Perry et al, 1997, Soave (1972)):

$$P = \frac{RT}{V-b} - \frac{a(T)}{V(V+b)} \quad (10)$$

$$where \quad a(T) = 0.4274\left(\frac{R^2T_c^2}{P_c}\right)\left\{1 + m\left[1-\left(\frac{T}{T_c}\right)^{0.5}\right]\right\}^2 \quad (11)$$

$$m = 0.480 + 1.57\omega - 0.176\omega^2 \quad (12)$$

$$b = 0.08664\frac{RT_c}{P_c} \quad (13)$$

The kinetic energy of turbulence, k and the turbulence dissipation term, ε are computed by solving the following two transport equations;

$$\frac{\partial}{\partial t}(\rho k) + \frac{\partial}{\partial x}(\rho V_x k) + \frac{1}{r}\frac{\partial}{\partial r}(r\rho V_r k) = \frac{\partial}{\partial x}\left(\left(\mu + \frac{\mu_t}{G_k}\right)\frac{\partial k}{\partial x}\right) + \frac{1}{r}\frac{\partial}{\partial r}\left(r\left(\mu + \frac{\mu_t}{G_k}\right)\frac{\partial k}{\partial r}\right) + S_k \quad (14)$$

$$\frac{\partial}{\partial t}(\rho \varepsilon) + \frac{\partial}{\partial x}(\rho V_x \varepsilon) + \frac{1}{r}\frac{\partial}{\partial r}(r\rho V_r \varepsilon) = \frac{\partial}{\partial x}\left(\left(\mu + \frac{\mu_t}{G_\varepsilon}\right)\frac{\partial \varepsilon}{\partial x}\right) + \frac{1}{r}\frac{\partial}{\partial r}\left(r\left(\mu + \frac{\mu_t}{G_\varepsilon}\right)\frac{\partial \varepsilon}{\partial r}\right) + S_\varepsilon \quad (15)$$

In the above equations, $S_k = \mu_t g - \rho\varepsilon$, $S_\varepsilon = C_1 g\mu_t\varepsilon k - C_2\rho\frac{\varepsilon^2}{k}$ and $\mu_t = C_\mu\rho\frac{k^2}{\varepsilon}$, $C_\mu = 0.09, C_1 = 1.4, C_2 = 1.92, G_k = 1.00, G_\varepsilon = 1.3, G_T = 0.85$, V_r and V_z are the radial and axial velocity components (m/s), k is the thermal conductivity (W/mK), ρ is density (kg/m^3), μ is dynamic viscosity (Ns/m^2), τ is shear stress (N/m^2) ; r, z and θ are the radial, axial and azimuthal directions respectively; T, P, t, C_p and q are temperature (K), pressure (N/m^2), time (s), constant pressure specific heat capacity $(J/kgK)$and heat flux (W/m^2)respectively.

3. NUMERICAL TECHNIQUE

The finite volume method is the numerical solution method adopted in this work. It is one of many methods that come under a general name - Computational Fluid Dynamics. In using the finite volume method, the general form of the conservation equations of fluid for the geometry considered in this work, for any scalar variable ϕ can be represented as follows;

$$\frac{\partial}{\partial t}(\rho\phi) + \frac{\partial}{\partial x}(\rho V_x\phi) + \frac{1}{r}\frac{\partial}{\partial r}(r\rho V_r\phi) = \frac{\partial}{\partial x}\left(\Gamma\frac{\partial\phi}{\partial x}\right) + \frac{1}{r}\frac{\partial}{\partial r}\left(r\Gamma\frac{\partial\phi}{\partial r}\right) + S_\phi \quad (16)$$

ϕ represents any of the variables, $V_r, V_x, T, k\ and\ \varepsilon$ while $\boldsymbol{\Gamma}$ represents μ and k. In employing the method, bracketed smaller contributions to the viscous stress terms in the transport equation are hidden (Versteeg and Malalasekera, 2007). Equations 1, 2, 3, 10, 15 and 16 are then integrated over a control volume after which Gauss' divergence theorem is applied to give the following;

$$\int_{CV}\frac{\partial}{\partial t}(\rho\phi)dV + \int_A n.(\rho V_x\phi)dA + \int_A n.(r\rho V_r\phi)dA = \int_A n.\left(\Gamma\frac{\partial\phi}{\partial x}\right)dA + \int_A n.\left(r\Gamma\frac{\partial\phi}{\partial r}\right)dA + \int_{CV}S_\phi dV \quad (17)$$

The solution region comprising of a grid is then divided into discrete control volumes (CV). The CV surface consists of four (in 2D) plane faces, denoted by lower-case letters corresponding to their direction (e, w, n, s) with respect to the central node (P) (Ferziger and Peric, 2012)

The governing equations are then integrated over the CV to obtain a discrete equation on node P. The equation is as follows;

$$\frac{\rho_p(\phi_p - \phi_p^0)\Delta V}{\Delta t} + (\rho V_x A\phi)_e - (\rho V_x A\phi)_w + (\rho V_r A\phi)_n - (\rho V_r A\phi)_s = \left(\Gamma A\frac{\partial\phi}{\partial x}\right)_e - \left(\Gamma A\frac{\partial\phi}{\partial x}\right)_w + \left(\Gamma A\frac{\partial\phi}{\partial r}\right)_n - \left(\Gamma A\frac{\partial\phi}{\partial r}\right)_s + (S_p\phi_p + S_u)\Delta V_p \quad (18)$$

The integration of the continuity equation also gives;

$$\frac{(\rho_p - \rho_p^0) r \Delta x \Delta r}{\Delta t} + (\rho U A)_e - (\rho U A)_w + (\rho V A)_n r - (\rho V A)_s r = 0 \quad (19)$$

In the discretization of the governing equations, implicit discretization was employed in the temporal terms. A time step of 2.85596×10^{-6} seconds was used. Implicit discretization for unsteady flows has the advantage of producing unconditionally stable results. Central differencing scheme was used in the spatial diffusion terms while second order upwind differencing scheme was employed in the spatial convection terms.

The general discrete equation is then;

$$a_P \phi_P = a_W \phi_W + a_E \phi_E + a_S \phi_S + a_N \phi_N + a_P^0 \phi_P^0 + S_U \quad (20)$$

where $a_P = a_W + a_E + a_S + a_N + a_P^0 + \Delta Fr - S_P$, $\Delta Fr = (F_e r - F_w r) + (F_n r - F_s r)$, $F_e = (\rho U)_e A_e$, $F_w = (\rho U)_w A_w$, $F_n = (\rho U)_n A_n$, $F_s = (\rho U)_s A_s$

In solving the above equation, the staggered grid arrangement was used. The reason for using staggered grid in solving pressure-velocity coupling equation is as a result of a uniform pressure field that would be obtained if velocity and pressure were stored at the same nodal points.

Next, a pressure-velocity calculation procedure, known as, Pressure-Implicit with Splitting of Operators (PISO) originally developed by Issa (1986) for the non-iterative computation of unsteady compressible flows was employed in the computation. It is a guess-and-correct procedure and has been adapted by Versteege and Malalasekera (2007) for steady flows. It involves one predictor step and two corrector steps. The method is an improvement to Semi-Implicit-Pressure Link Equation (SIMPLE) algorithm originally invented by Patankar and Spalding (1972) in the sense that it has an additional corrector step to enhance it. Furthermore, it is efficient and fast (Versteege and Malalasekera, 1995).

Boundary conditions

The boundary conditions for gas flow in pipeline in a 2D geometry are as shown in Figure 1.

Steady state condition

- *Fluid boundaries:*
  a. Inlet: P, u *and* T are defined and ρ is defined by state equation.
  b. Outlet: general condition of fluid which is almost commonly applied in finite volume method is as follows (Versteeg and Malalasekera, 1995, Noorbehesht,2012):

$$\frac{\partial T}{\partial n} = 0 \text{ and } \frac{\partial u_n}{\partial n} = 0$$

And a defined P_{out} aiming considered mass flow rate, and n is the normal outward vector of outlet surface.

- *Solid boundary:*

No slip condition; $u = u_w = 0$

Constant temperature on the wall; $T = T_w$

Symmetric boundary condition; $\frac{\partial \phi}{\partial n} = 0$

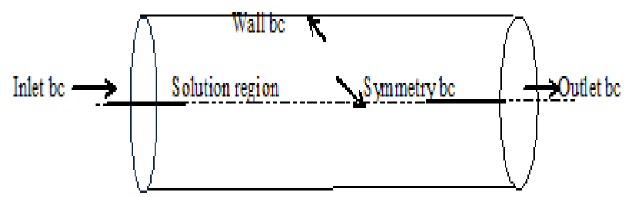

Figure 1: Flow domain and boundary conditions (Noorbehesht, 2012)

Initial Conditions for Unsteady State

The parameters P, u, T *and* ρ must be specified according to their initial values at $t = 0$ Therefore, the steady state condition data are also the initial conditions of the unsteady state.

Operating *Conditions*;

Pipe diameter D = 0.35m, pipeline length L = 500m; inlet pressure $P_{in} = 26337.01Pa$; outlet pressure $P_{out} = 20574.05Pa$; inlet temperature $T_{in} = 46.86$ ºC ; outlet temperature $T_{out} = 34^oC$; *Physical properties of gas*; the current properties of the gas are assumed constant. Molecular weight $M_w = 19$; thermal conductivity k = $0.0332\ W/mK$; specific heat at constant pressure $C_p = 2530\ J/kgK$;; viscosity, μ = $1.56 \times 10^{-5}\ kg/ms$.

4 RESULTS

Model Validation and Simulation

To validate the model, pressure data published by Noorbehesht (2012) which he obtained from the National Iranian Gas Company for the validation of a model he proposed were used. The pipeline he considered for simulation was 135km in length. Inlet and outlet pressures were 71.11bar and 55.55bar respectively while inlet and outlet temperatures were 46.86^{o}C and 34^{o}C respectively. For the purpose of validation of the model considered in this work, this pipeline length was scaled down to 500m. The scale factor was calculated by the method of geometric similarity presented by Rajput (1998). It was then used to obtain the inlet and outlet pressure values stated above (i.e. $26337.01 Pa$ and $20574.05 Pa$). The temperatures employed in the present simulation remained 46.86^{o}C at the inlet and 34^{o}C at the outlet. Steady state results were first obtained and then used as initial conditions for the unsteady state simulation. ANSYS FLUENT, a finite volume simulation software was used for simulation. The profile for pressure is similar to that obtained by Noorbehesht (2012). This proves the accuracy of the solution used for the model. Profiles for temperature, density, velocity, along the pipeline were also obtained. They are presented below.

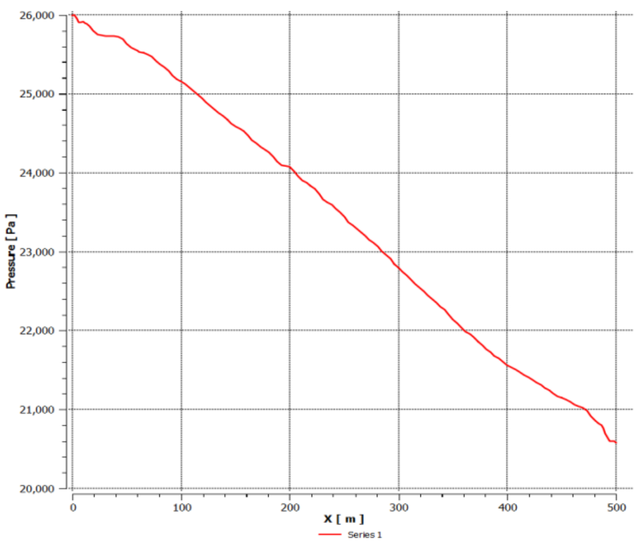

Figure 2: Graph of pressure distribution along the length of the pipeline

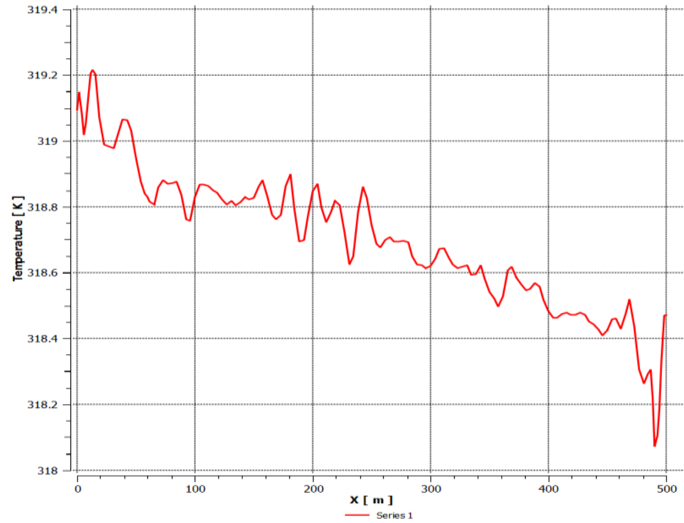

Figure 3: Graph of temperature distribution along the length of the pipeline

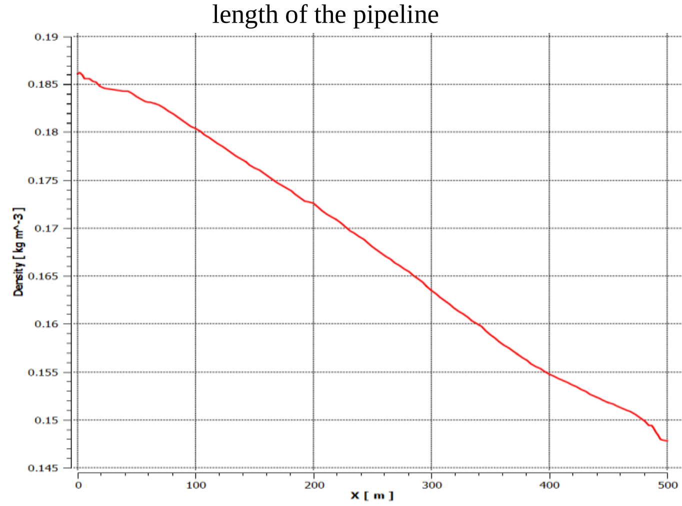

Figure 4: Density distribution along the pipeline length

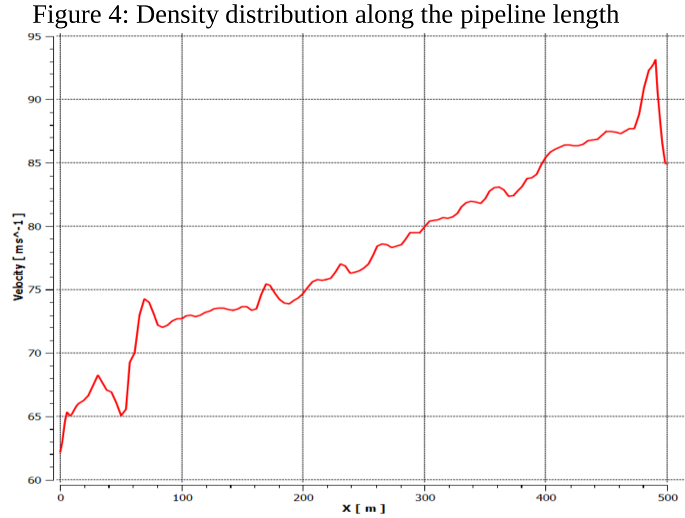

Figure 5: Velocity distribution along the length of the pipeline

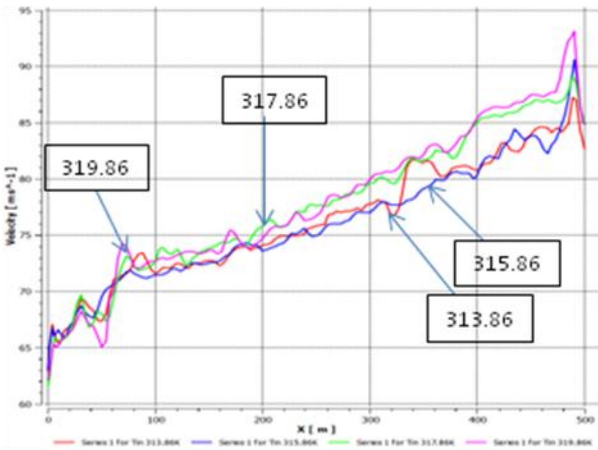

Figure 6: Variation of velocity along the pipeline length at different inlet temperatures

5. DISCUSSIONS

Figure 2 above shows a plot of the distribution of pressure along the pipe at transient condition. A drop in pressure from 26,000Pa at the pipe entrance to 20,600Pa 500m downstream of the pipe can be seen. This is to be expected since for a fluid flowing down a conduit, there's usually a pressure drop due to frictional resistance. The plot shows same trend as that obtained by Noorbehesht (2012), Noorbehesht and Ghaseminejad (2013), Nouri-Borujerdi (2011). The Figure 3 above shows a plot of the temperature distribution in the pipe at transient condition. There is also a decrease in temperature. This trend is the same as that of the pressure as can be seen since from the equation of state, pressure is directly proportional to temperature (Perry et al, 1997; Bansal, 2008).

Figure 4 and Figure 5 show plots of density and velocity respectively. It can be seen that density decreases along the length of the pipeline while the velocity plot shows a reverse trend. This is in consonance with the mass flow rate equation shown below (which shows that velocity increases with density decrease);

$$m = \rho u A \qquad (21)$$

Where $m = mass\ flow\ rate., kg/s\ , \rho = density\ of\ gas, kg/m^3,\ u = axial\ velocity, m/s$ $and\ A = cross - sectional\ area\ of\ pipeline, m^2.$

Figure 6 shows variation of velocity of gas with inlet temperature along the pipeline. Inlet velocity increases due to inlet temperature increase. The inlet temperatures include 313.86K, 315.86K, 317.86K and 319.86K. The increase of course stems from the fact that motion of gas molecules (hence their velocity) increases as temperature increases in a given system (Noorbehesht, 2012). This same trend is seen towards the end of the pipeline though the velocity values for the 315.86K and 317.86K inlet temperatures tend to be the same.

6. CONCLUSIONS

A method for predicting flow properties in a natural gas pipeline has been presented in this work. First, transient compressible natural gas flow was modeled via the continuity, momentum and energy equations together with the $k - \varepsilon$ turbulence equations. The real gas Soave-Redlich-Kwong equation was included as an auxiliary equation. The method of simulation involved the use of the PISO algorithm on a staggered grid. ANSYS FLUENT was then used to carry out the simulation. The results of the simulation show that the method employed is adequate for predicting flow properties in a pipeline system. The method can be employed by the Oil and Gas industries for the knowledge/control of natural gas pipeline system behaviour.

REFERENCES

Bansal, R. K., (2008). A Textbook of Fluid Mechanics, (p. 19). Laxmi Publications (P) Limited, New Delhi.

Blazek, J., (2001). *Computational Fluid Dynamics: Principles and Applications*. Elsevier.

Behbahani-Nejad, M and Bagheri, A., (2008). A MATLAB Simulink Library for Transient Flow Simulation of Gas Networks. *World Academy of Science, Engineering and Technology*, 19.

Bird, R. B., Stewart, W. E. and Lightfoot, E, N., (2002). *Transport Phenomena* (p. 337). John Wiley and Sons, Inc.

Ferziger, J. H. and Peric, M., (2002), Computational Methods for Fluid Dynamics. Springer. 3rd edition.

Issa, R. I., (1986). Solution of Implicitly Discretised Fluid Flow Equations by Operator-Splitting. *J. Comput. Phys.*, 62, 40–65.

Kessal, M., Boucetta, R., Zamoum, M. and Tikobaini, M., (2014). Numerical Modelling of transients in gas pipeline. *International Journal of Physical Sciences*, 9(5), 82-90.

Noorbehesht, N., (2012). Numerical Simulation of Natural Gas Flow in Transmission Lines through CFD Method

Considering Effective Parameters. *J. Basic. Appl. Sci. Res.*, 2(8), 7473-7487.

Noorbehesht, N. and Ghaseminejad, P., (2013). Numerical Simulation of the Transient Flow in Natural Gas Transmission Lines Using a Computational Fluid Dynamic Method. *American Journal of Applied Sciences*, 10 (1): 24-34.

Nouri-Borujerdi, A. and Ziaei-Rad, M., (2007). Numerical Prediction of Developing Flow in Gas Pipelines. *5th International Conference on Heat Transfer, Fluid Mechanics and Thermodynamics.*

Nouri-Borujerdi, A. and Ziaei-Rad, M., (2010). Numerical Modeling of Transient Turbulent Gas Flow in a Pipe Following a Rupture. *Transaction B: Mechanical Engineering*, 17(2), 108-120. © Sharif University of Technology, Tehran, Iran.

Nouri-Borujerdi, A., (2011). Transient modeling of Gas Flow in Pipelines following catastrophic failure. *Mathematical and Computer Modeling*, 54, 3037–3045.

Perry, R. H., Green, D. W. and Maloney, J. O., (1997). Perry's Chemical Engineers' Handbook, Seventh Edition (p. 4-21). McGraw-Hill.

Rajput, R.K., (1998). Fluid mechanics and Hydraulic Machines, S Chand and Company Limited.

Soave, G. (1972). Equilibrium constants from a modified Redlich-Kwong equation of state. Chemical Engineering Science. 27(6), 1197-1203.

Siögreen B., (1995). High Order Centered Difference Methods for the Compressible Navier-Stokes Equations. *Journal of Computational Physics*, 117, 67-78.

Versteeg, H K and W Malalasekera, W., (1995). *An introduction to computational fluid dynamics the finite volume method, First edition*. Longman Scientific and Technical.

Versteeg, H K and W Malalasekera, W., (2007). *An introduction to computational fluid dynamics the finite volume method, second edition*. Longman Scientific and Technical.

NOMENCLATURE

V_r	Velocity in the radial (r) direction, m/s
V_z, U, u	Velocity in the axial (z) direction, m/s
r	Radial direction
x, z	Axial direction, m
T	Temperature, K
t	Time, s
E	Total internal energy, J
k	Thermal conductivity, W/mK
$k,$	Kinetic energy of turbulence, J/kg
m	Mass flow rate, kg/s
A	Cross-sectional area, m^2
P	Pressure, N/m^2
L	Pipeline length, m
V	Volume, m^3
D	Pipeline diameter, m
C_p	Constant pressure specific heat capacity, J/kgK
q	Heat flux, W/m^2
g	Acceleration due to gravity, m^2/s
$\bar{Z}$	Average value for compressibility factor
R	Gas constant
Greek Characters	
μ	Dynamic viscosity, Ns/m^2
ρ	Density, kg/m^3
τ	Shear stress tensor, N/m^2
θ	Azimuthal direction
ε	Turbulence dissipation rate, m^2/s^3